GEM TN-93-392

TTR Test Results of a UH CSC Prototype

K. Lau, B. Mayes, J. Pyrlik, and R. Weinstein
Institute for Beam Particle Dynamics
University of Houston
Houston, TX

Yu. Bonushkin, A. Gonzales,† L. Villasenor,† and G. Yost
Superconducting Super Collider Laboratory
Dallas, TX

August 6, 1993

Abstract;

An open profile CSC prototype was constructed and tested at the Texas Test Rig (TTR) using cosmic ray muons. Construction details and test results are reported. The single-layer resolution was measured to be 40-60 μ m, depending on the high voltage and the azimuthal angle of the muon, which meets the GEM muon chamber resolution requirement.

GEM TN-93-392
August 6, 1993

TTR Test Results of a UH CSC Prototype

K. Lau, B. Mayes, J. Pyrlik, and R. Weinstein

Institute for Beam Particle Dynamics
University of Houston
Houston, Texas 77204-5506

Yu. Bonushkin, A. Gonzalez,† L. Villasenor,† and G. Yost

Superconducting Super Collider Laboratory
Dallas, Texas 75237

Abstract

An open profile CSC prototype was constructed and tested at the Texas Test Rig (TTR) using cosmic ray muons. Construction details and test results are reported. The single-layer resolution was measured to be 40-60 μm, depending on the high voltage and the azimuthal angle of the muon, which meets the GEM muon chamber resolution requirement.

1. Introduction

Cathode strip chambers (CSC) are a leading contender for the GEM muon detector technology. The principles of operation and merits are described in Ref. 1. The precision coordinate is measured along an anode wire by locating the centroid of the charge induced on the cathode strips which run orthogonally to the wires. The precision elements are, therefore, the strips. Two approaches appear in the literature.[2-5] In most cases, the anode wires are constructed as in multiwire proportional chambers (MWPC).[2,3] In this approach, the wires have to be accurately placed in order to avoid electrostatic instability. A more robust approach is to replace the wire planes by modular wire chambers in which the anode wires are isolated by conductive walls.[4,5] For example, the chambers could be constructed from open profiles in which the wires are strung along a U-shaped conductive profile. The profile is sealed in a nonconductive gas envelope. The charge is induced on cathode strips placed on top of the the open side of the channels. For this field configuration, the positioning of the anode wires is less critical, roughly by about a factor of 5-10.[6]

The spatial resolutions of CSC's based on Iarocci-type open profiles reported in the literature are typically an order of magnitude worse than that of MWPC CSC's.[4,5] The main reason for the inferior resolution is that the graphite coating commonly employed in standard Iarocci-type PVC streamer chambers has a typical resistivity of 200 k$\Omega/\square$, which causes a long RC time for the signal and a degradation of the signal due to non-uniformity of the graphite coating.

Recent work by Korytov *et al.*[7] using graphite-coated Al open profile CSC with 1 cm strips achieved spatial resolution of about 100 μm in a 0.5 TeV muon beam. It is therefore natural to explore the performance of CSCs based on Iarocci-type open profile CSCs with low cathode resistivity. If it is shown that resolutions comparable to or better than 75 μm can be achieved, this approach provides an inexpensive way to construct the GEM muon chambers. Further advantages of this approach are described in Ref. 8.

The Houston group constructed a medium-sized (0.5 m x 1.0 m) CSC prototype based on Iarocci-type modular chambers, and studied its performance using cosmic ray muons. The major improvements over previous attempts are :

a. The cathode strips were made with high precision such that they are not the limiting factor in the resolution.

b. The resistivity of the graphite coating on extruded PVC profiles is controlled by

applying multiple coatings to attain both high uniformity (< 10% variation rms) and low resistivity ($\simeq$ 4 k$\Omega/\square$).

This report summarizes our preliminary results. Details of the construction are given in section 2. The cosmic ray test results are described in section 3.

2. The UH Prototype

2.1 The Mechanical Construction

A side view of the prototype is shown in Fig. 1. It consists of 3 layers of precision strip boards which are made out of commercial copper-clad FR-4 boards. (FR4 was chosen for its fire-retardant property. For the final GEM application, due to the large neutron capture cross section of Bromine, an ingredient of FR-4, other substrate such as G10 may be more appropriate.) The thickness of the copper is about 17 μm (0.5 oz/sq. ft.). The thickness of the strip boards was measured to be 1.53 $\pm$ 0.01 mm. A schematic of the copper strip pattern is shown in Fig. 2 where the tolerances are also indicated. The copper strips are 4.00 mm wide and 1000.00 mm long. The strip width tolerance was specified to be $\pm$ 25 μm across the 0.5 m width. The design also included fiducial marks on the board which are used for external survey references.

Three boards were manufactured by Microwave Printed Circuitry (MPC) at Lowell, MA using standard photo-etching techniques. The manufacturing process is described briefly as follows. An optically-precise ($\pm$ 1 μm) pattern of the design is first produced on a Mylar-based photographic film. The copper surface, which is dip-coated with a liquid photo-resist is exposed to UV light. The copper strips are masked by the film. The exposed copper is etched by standard chemical techniques. The expected precision of this technique is of the order of the thickness of the copper due to the etching process. We surveyed two of the three boards produced and found the tolerance to be within our specifications.[9] Most importantly, the measured data showed a strip pitch constant to within 1 μm. Hence, the center of each strip can be located to better than 50 μm over a distance of 50 cm. Fig. 3 is a plot of the difference between the measured and expected (calculated assuming a constant pitch) strip center positions. The measured pitch was 4999 $\pm$ 13 (stat.) $\pm$ 1 (syst.) μm. The random error includes measurement errors. The 1 μm difference between the observed pitch and the design value (5000 μm) is probably due to temperature, humidity,

and relative length calibration uncertainties.

Each strip board was epoxied onto a 2'x 4'x 1/2" honeycomb panel for rigidity. The three honeycomb panels were derived from a single 4' x 8' x 1/2" honeycomb panel obtained from NORDAM as a standard off-the-shelf item. The composition of the panel is listed in Table 1. The actual thickness of the panels was measured to be 0.482 ± 0.003 " (12.24 ± 0.08 mm). The observed flatness far exceeded our expectation, but this is not essential to our design.

The strips were aligned by inserting a precision rod through four precision holes drilled through Al inserts in the panels. Two of the holes are 1/2" in diameter and the other two are of racetrack design with two 1/2" holes separated by 25 μm, to allow for possible unequal thermal expansion of the panels. (The thermal expansion coefficient of the panel was quoted to be 10-14 ppm/C°.) The position of the holes is precisely referenced to the fiducial marks etched on the strip boards. To provide mechanical strength for the holes, a 1" x 1" x 1/2 " Al block was inserted and epoxied in each corner of the panels. The holes were machined through the Al blocks. This procedure was accomplished by standard techniques in the UH machine shop. The expected alignment accuracy was 50 μm. The alignment error determined by straight-through muons is about 30 μm. (See section 3.4c.)

Twelve 26" (660 mm) long standard Iarocci-type chambers (eight 1cm x 1cm cells per chamber) were sandwiched between every two panels. The chambers were aligned perpendicular to the strips without staggering to ± 0.5 mm; the error in perpendicularity introduces an error of about 5 μm to the spatial resolution. The chamber-panel assembly was supported on a 1" Al honeycomb panel.

The open profile chambers were constructed by the production-line method at the Streamer Chamber Assembly and Research Facility at the University of Houston. By applying multiple graphite coatings, the average resistivity was set to about 4 kΩ /□. The resistance spectrum for 320 samplings, taken every 10 cm along each profile, is shown in Fig. 4. The fractional variation of the resistivity is about 10%. The chambers were strung with 44.5 μm (1.75 mil) gold-plated tungsten wires with a tension of about 120 g, and the wires were anchored at both ends by soldering onto a G10 board. The vertical placement precision of the wires is controlled by plastic end pieces to ± 0.1 mm. The largest error in the wire position comes from the uncertainty of the profile within the sheath, which is

estimated to be ± 0.2 mm. However, calculations indicate that this level of vertical wire displacement error does not degrade the resolution significantly.[6]

2.2 Readout Electronics

The middle 10 strips of each layer were connected to charge amplifiers, one channel for each strip. Thirty-two low noise (2000 electron-equivalent) amplifiers were designed and built by a group at DUBNA.[10] The overall charge gain was optimized to be about 2000 for our application. The output for a test pulse of characteristics similar to those of a chamber pulse (10 ns rise time and 100 ns fall time) is shown in Fig. 5. It is evident that the fall time of the output pulse is well within 500 ns, and therefore a signal integration time of 500 ns is adequate for our measurements. The strips are connected to the amplifiers via short ($\simeq$ 20 cm) 50-ohm RG174 coaxial cables. The 32 amplifiers were housed in two Al boxes, each 32 cm x 12.5 cm x 12 cm. The 16 amplifiers within a box share common low voltage power (± 12 V) and test pulses. The test pulses are reduced by a factor of 2000 before they are distributed to the amplifiers. The outputs from the amplifiers were routed via 50 m RG 174 coaxial cables to three 12-channel charge-integrating ADCs (Lecroy 2249 W). The cable length was chosen to provide a delay of 250 ns in order to match the timing of the cosmic ray trigger. The measured delays of the cables are within 2 ns. An attenuation of about a factor of 2 in amplitude was observed in signals in the 50-m long cables.

The amplifiers were calibrated by test pulses between runs whenever the running conditions changed. The test pulses, generated by a HP model 8082A pulse generator with a rise time of 10 ns and a fall time of 100 ns to simulate the chamber pulses, are injected into each amplifier box via a 50 m RG 174 coaxial cable. The calibration data were recorded on the ADCs for several input amplitudes to determine the relative gain of the channels. The measured relative gains are shown in Fig. 6, where their values are normalized to 1. We found that the relative gains remained constant throughout the 2-month data-taking period.

The high voltage (HV) for the chambers, in groups of 12, was supplied by a Bertan model 375P power supply. The typical current for each group of 12 chambers is 10 nA. The power to the amplifiers was supplied by 2 Lambda model LQ-521 power supplies.

3. TTR Test Results

3.1 TTR

For the purpose of testing and comparing different muon chamber technologies, a cosmic ray test facility, the Texas Test Rig (TTR), was constructed at the SSCL[11]. The total space available for testing is contained in a frame of 1.2 m (width) x 4.5 m (length) x 3.0 m (height), arranged in multiple shelves. Two scintillator hodoscope planes, located at the top and the bottom of the TTR, respectively, provide accurate timing ($\pm$ 0.5 ns) for cosmic ray muons passing through the test volume. Four planes of Iarocci chambers, two in each coordinate, with digital readout of 1 cm strips are used for the tracking of the muons. A large electromagnet with 1-m thick iron is located at the bottom of the structure for muon momentum determination. The bending power of the magnet, combined with tracking information from the Iarocci chambers, provides momentum discrimination up to 10 GeV/c. In addition, the minimum energy required to penetrate the 1 m steel of the magnet is about 1.3 GeV. The multiple Coulomb scattering of 1.5 GeV/c muons in the UH prototype contributes about 17 μm to the resolution, which is completely negligible. Since the TTR trigger requires the muons to penetrate the 1.0 m steel, providing adequate resultant momentum selection, all the data were taken with the magnet switched off.

3.2 Data

The UH prototype was intalled at the TTR from August to December, 1993, in the upper-most shelf of the TTR. The chambers were operated with a gas mixture of 25% argon and 75% isobutane with a typical flow rate of 0.25-0.5 liters/min. For reliable proportional mode operation, the HV was limited to 3.3 kV. The chamber begins to go into streamer mode when the HV is above 3.5 kV.

The trigger logic requires a coincidence of one of the two top scintillators in the middle and one of the six bottom scintillators. A typical trigger rate is 10 Hz, which is consistent with the geometric acceptance of the prototype for muons above 1 GeV. This trigger generates a 500 ns gate which preceeds the earliest chamber signals by about 100 ns for the ADCs . The events were recorded by a VME-based DAQ system run on a Sun workstation.

During the data-taking period, about 400,000 triggers were recorded, roughly equally

divided at 3 different HV settings: 3.1, 3.2, and 3.3 kV.

3.3 Analysis Procedure

Since the triggers consist mostly of muons going through the non-instrumented area of the prototype (only 10 out of the 100 strips in each layer are instrumented), a fast offline filter program was run on the Sun workstation to weed out events in which less than 100 raw ADC counts were observed in all strips in all three planes. About 3% of the events passed the fast filter which were sent to UH for further analysis.

The analysis is aided by a display program which plots the corrected pulse heights for each strip. Fig. 7 is an event in which a muon passed through the instrumented region. The number of strips with significant counts in each layer is typically 3 to 4.

We used a subset of the raw events to determine the pedestals for each channel. Shown in Fig. 8 is a typical pulse height distribution for all triggers. The peak corresponds to the pedestal, and the width is a measure of the noise level of that channel. Real data counts are off the high end of the figure. Typical pedestal and noise levels are 30 and 5 ADC counts, respectively. The noise level agrees with the expected noise from the strips and amplifiers.

Prior to reconstructing the muon tracks in the prototype, the following cuts and corrections were applied to the data.

a. The pedestal-subtracted ADC counts were corrected for gain variation.
b. Events with at least one channel exceeding the dynamic range of the ADC (1900 counts) were excluded.
c. A fiducial cut, which excludes the two outermost strips in each layer, was applied.

3.4 Results

a. Pulse Height Distribution

The pedestal-subtracted and gain-corrected pulse heights are shown in Fig. 9 as a function of the HV. Since events with at least 1 ADC-overflow were not included in the analysis and only pulse heights of 4 strips are summed, the spectra cannot be directly compared with the standard Landau distribution.[12] Monte Carlo simulation studies which include these cuts are in progress.

The ADC-overflow events, which are excluded from the analysis, are presumably caused by the production of a high energy δ-ray. The ADC-overflow condition corresponds to an energy of > 10 keV for the δ-electron. The observed ADC-overflow fraction of 3% per plane is consistent with prediction if contributions from the chamber walls are included.[12]

There is also a small percentage of events in which the pulse height from one of the planes is anomalously low. We attribute these events to muons going through the inactive areas between two adjacent chambers. We estimated from geometry the fraction to be 4 $\pm$ 1 %, which agrees with our data.

We showed in Fig. 10 the mean pulse height as a function of HV, V. The data points were fitted to the standard gain-versus-voltage formula,[13]

$$G = ke^{\gamma V},$$

where the gain, G, is defined to be proportional to the mean pulse height. The solid curve is the best fit, corresponding to $k = 0.4855$ and $\gamma = 0.002508$ V^{-1}. The fractional change in gain as a function of change in HV,

$$\frac{\Delta G/G}{\Delta V/V} = \gamma V \simeq 8.0.$$

b. Single-layer Resolution

We fitted the muon trajectories to a straight-line, and determined the single-layer resolution from the residuals. The charge centroid for each plane was determined by an algorithm based on a weighted average of the charge center-of-gravity (c.o.g.) using three and four strips.[2] Specifically, the charge centroid (x) is given by

$$x = (1 - \frac{2x}{w})x^{(3)} + \frac{2x}{w}x^{(4)}, \tag{1}$$

where $x^{(3,4)}$ are the charge c.o.g. using 3 and 4 strips, respectively, and w is the width of the strip. x is the coordinate perpendicular to the strips. Due to the finite width of the strips, the algorithmic centroid is different but correlated with the actual avalanche position. This particular weighting scheme ensures that x is exact at $x = 0$ ($x = x^{(3)}$) and $x = w/2$ ($x = x^{(4)}$). Monte Carlo simulation showed that the residual systematic variation in between ($0 \geq x \geq w/2$) can be parametrized by

$$x_{corr} - x = A[sin\frac{2\pi x}{w} - 0.077sin\frac{4\pi x}{w} + 0.041sin\frac{6\pi x}{w}], \tag{2}$$

where x_{corr} is the true avalanche position.[6] The amplitude, A, was determined by Monte Carlo calcualtion to be about 117 μm for tracks at normal incidence. However, we used the experimental data to determine the best value for A. The centroids found by the algorithm (1) were fitted to a straight-line. The residuals for the middle plane before correction are shown in Fig. 11a, as a function of x. As one can see, the residuals exhibit a periodic systematic variation with a period which agrees with the pitch of the strips. We applied a correction of the form given by (2) to the centroids. We allowed A to vary. We obtained the best resolution with $A \simeq 90$, and the resolutions were found to be quite insensitive to A. We also allowed in our fit to have a systematic misalignment among the three layers. (See section 3.4c.) The residuals of the best fits are shown in Fig. 11b, as a function of x. As one can see, the resolution is improved significantly, and is independent of x after the correction.

Due to statistical fluctuations of the ionization along the path of the muon, the charge centroid of an inclined track has an additional error of

$$\sigma_\phi = \frac{a \times tan\phi}{\sqrt{12N}},$$

where a is the height of the chamber and N is the number of primary ionization clusters. The average number of ionization clusters for our gas mixture, N, is 42[13]. ϕ is the angle between the wire and the muon track, projected onto a plane which contains the wire and is perpendicular to the strips. This angular degradation is to be added, in quadrature, to the resolution of tracks at normal incidence (σ_o). That is,

$$\sigma(\phi) = \sqrt{\sigma_o^2 + \sigma_\phi^2}. \tag{3}$$

The trigger limits ϕ to about $\pm$ 8°, as shown in Fig. 12. Due to limited statistics, we were not able to carry out a detailed study of the resolution as a function of ϕ. We report here the resolutions for normal incident tracks, $|\phi| \leq 2°$, and for $|\phi| \leq 6°$.

The resolutions for normal incident tracks are shown in Fig. 13 as a function of HV. The single-layer resolution is well-below the GEM specification of 75 μm. The resolution at 3.3 kV (38 $\pm$ 3 μm) surpassed the best published results.[3,4] The HV dependence of

the resolution is in agreement with contributions from electronic noise (estimated to be $\simeq$ 60 μm at 3.1 kV and assumed to fall as the inverse of the averge pulse height), intrinsic resolution due to the finite range of the ionization electrons ($\simeq$ 20 μm), and multiple Coulomb scattering ($\simeq$ 17 μm). More detailed analysis of systematic effects is in progress.

The resolutions most relevant to GEM, corresponding to $|\phi| \leq 6°$, are shown in Fig. 14. Again, the resolutions met the GEM requirement of 75 μm. The predicted average resolutions for this angular interval based on (3), assuming a constant muon flux, are in rough agreement with the data.

c. Alignment

Our fitting procedure allows the systematic shift of the middle layer strips relative to the top and bottom layer strips to be determined. Our results showed that a shift of 33 $\pm$ 3 μm existed. This level of alignment accuracy is consistent with our construction and alignment techniques.

4. Acknowledegements

We thank the technical staff at the University of Houston, especially C. Bell, D. Hungerford, and D. Parks for their assistance in the construction of the prototype. We also thank the staff of the SSCL for stable operation of the TTR and technical assistance during testing. We also benefited from useful discussions with V. Glebov, K. McFarlane, C. Milner, and G. Mitselmakher of the SSCL. K.L. wishes to thank A. Korytov and G. Mitselmakher for discussing their CSC prototype beam test results at FNAL prior to publication. We also thank F. Taylor and M. Marx, the GEM muon group leaders, for helpful discussions. This research was supported by the Department of Energy and the Texas National Research Laboratory Commission.

5. References

† Present address : *Universidad de Guanajuato, Mexico.*

1. GEM CSC Group, *The GEM Muon System Based on Cathode Strip Chambers,* GEM TN-92-199, October, 1992.
2. G. Charpak *et al.*, NIM **167**, (1979)455.
3. L. S. Barabash *et al.*, NIM **A236**, (1985)271.

4. G. De Agostini *et al.*, NIM **A252**, (1986)431.
5. G. Bauer *et al.*, NIM **A260**, (1987)101.
6. K. Lau, GEM TN-92-242.
7. N. Khovansky *et al.*, *Spatial Resolution Achievable with External Pick-up Strips,* (to be published).
8. K. Lau, B Mayes, J. Pyrlik, and R. Weinstein, *Proposal to Use Separated Profile Strip Chambers for the GEM Muon System* , GEM TN-93-281.
9. K. Lau, GEM TN-92-133.
10. M. O. Deighton, NIM **58**, (1968) 201; R. A. Boie *et al.*, NIM **192**, (1982) 365; P. D'Angelo *et al.*, NIM **193**, (1982)523.
11. E. Cas Milner *et al.*, *Overview of the GEM Muon System Cosmic Ray Test Program at the SSCL*, to be published in proceedings of the IISSC of May, 1993, San Francisco, California.
12. L. Landau, J. Phys. (USSR) **8**, (1944) 201.
13. F. Sauli, *Principles of Operation of Multiwire Proportional and Drift Chambers,* CERN Report 77-09 (1977). Reprinted in *Experimental Techniques in High Energy Physics,* edited by T. Ferbel, Addison-Wesley, 1987.

Table 1. The composition of honeycomb support panels

Item	Material	X_o (cm)	Thickness (cm)	Radiation length
Upper Skin	Epoxy Glass	19.4	0.051	0.0026
Core	NOMEX†	1400	1.123	0.0008
Lower Skin	Epoxy Glass	19.4	0.051	0.0026

† 3.0 lb/ft^3, 1/8 Cell honeycomb

UH
CSC Prototype

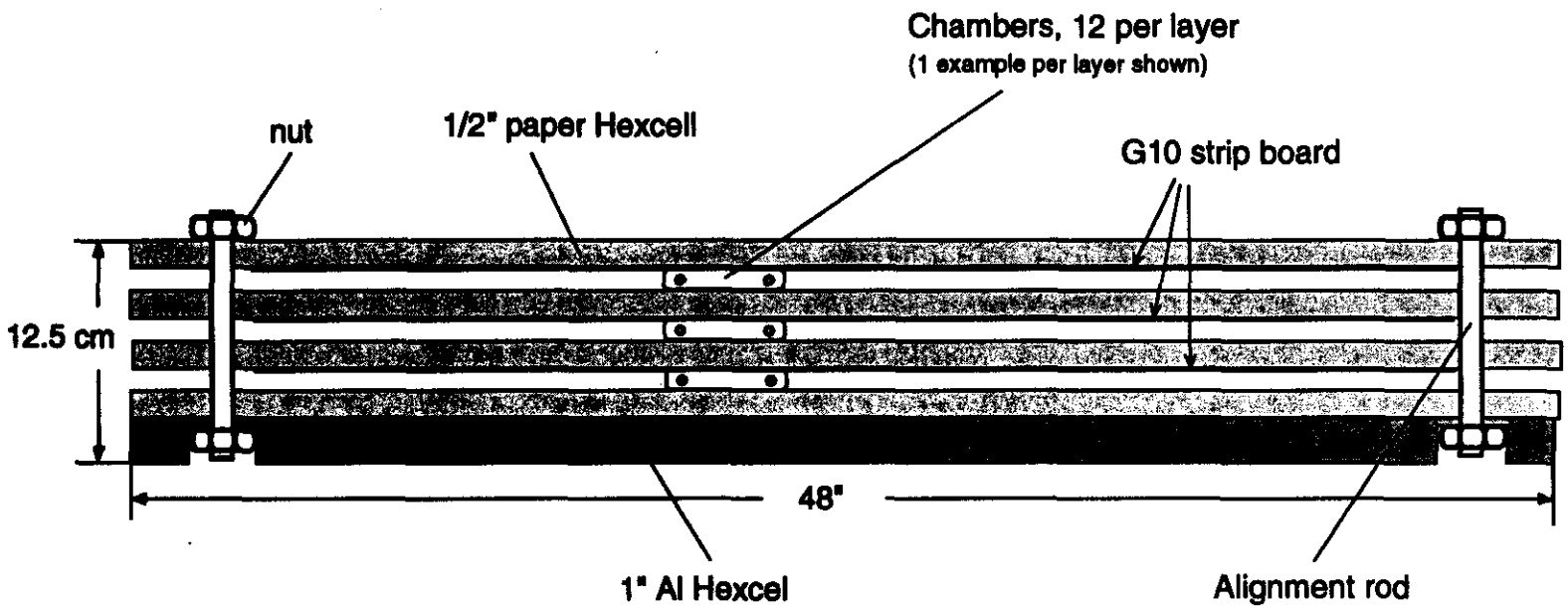

Figure 1. Side view of the UH CSC prototype.

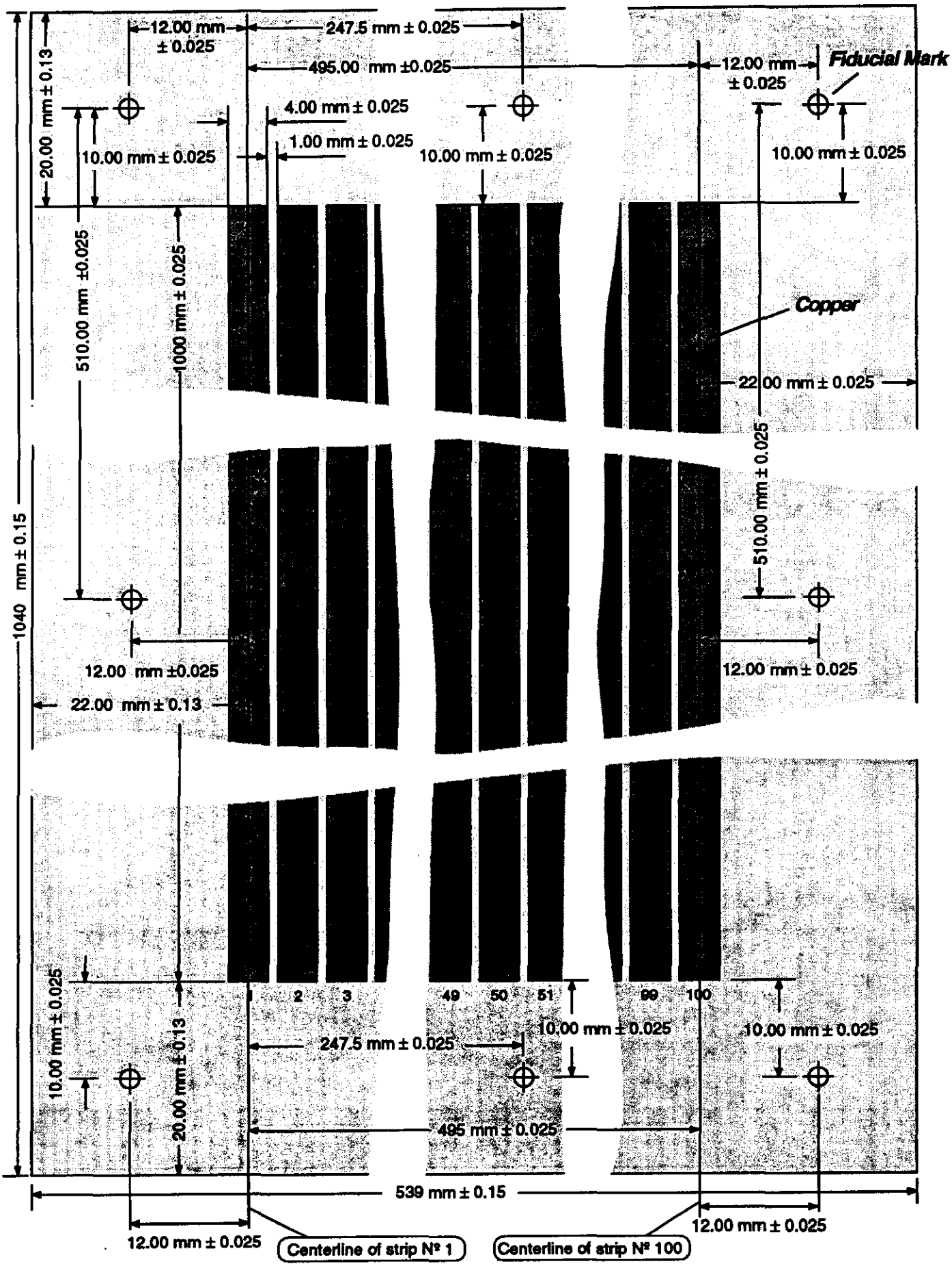

Figure 2. Schematic of the strip readout boards

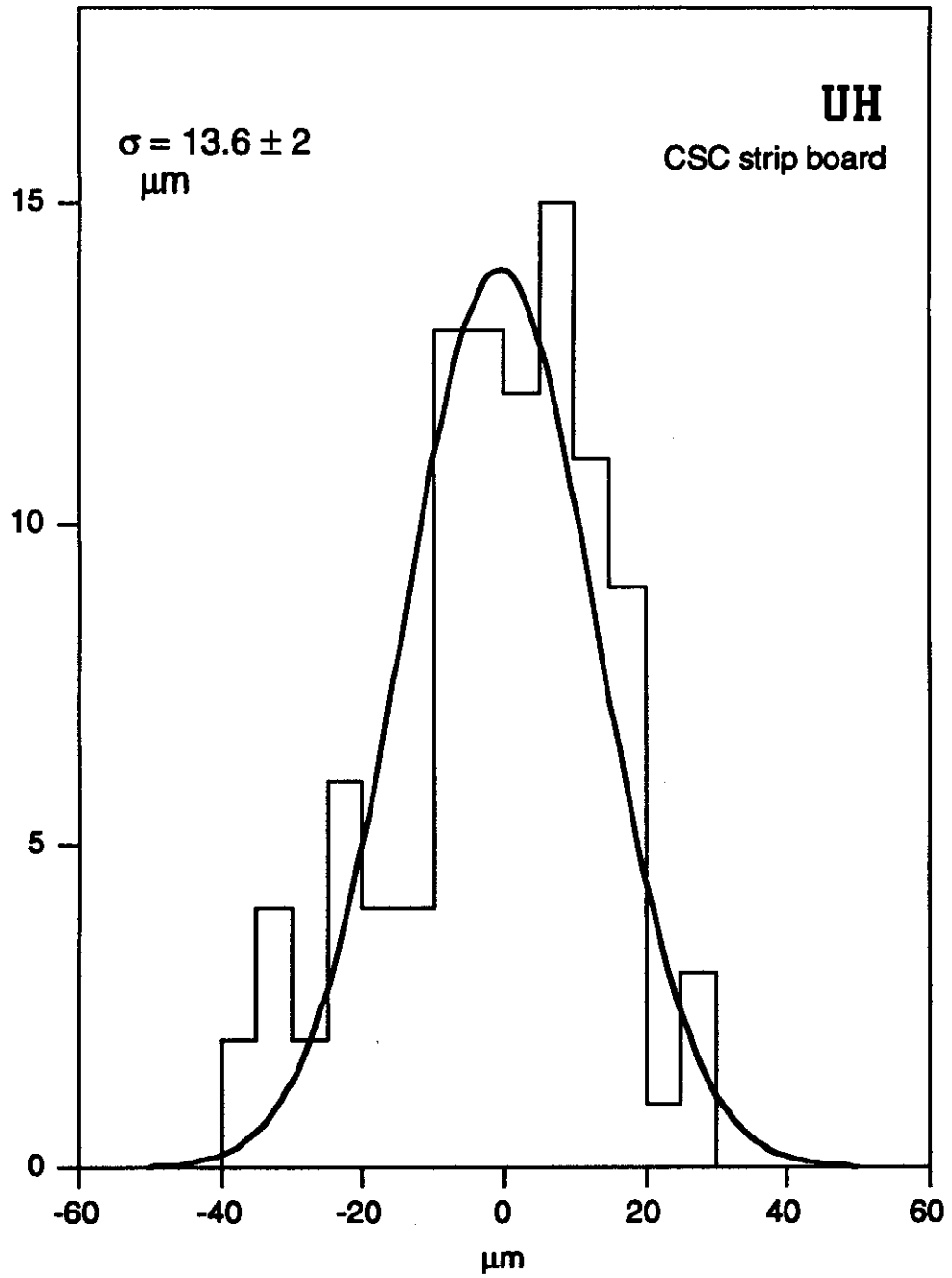

Figure 3. Residuals of strip centers

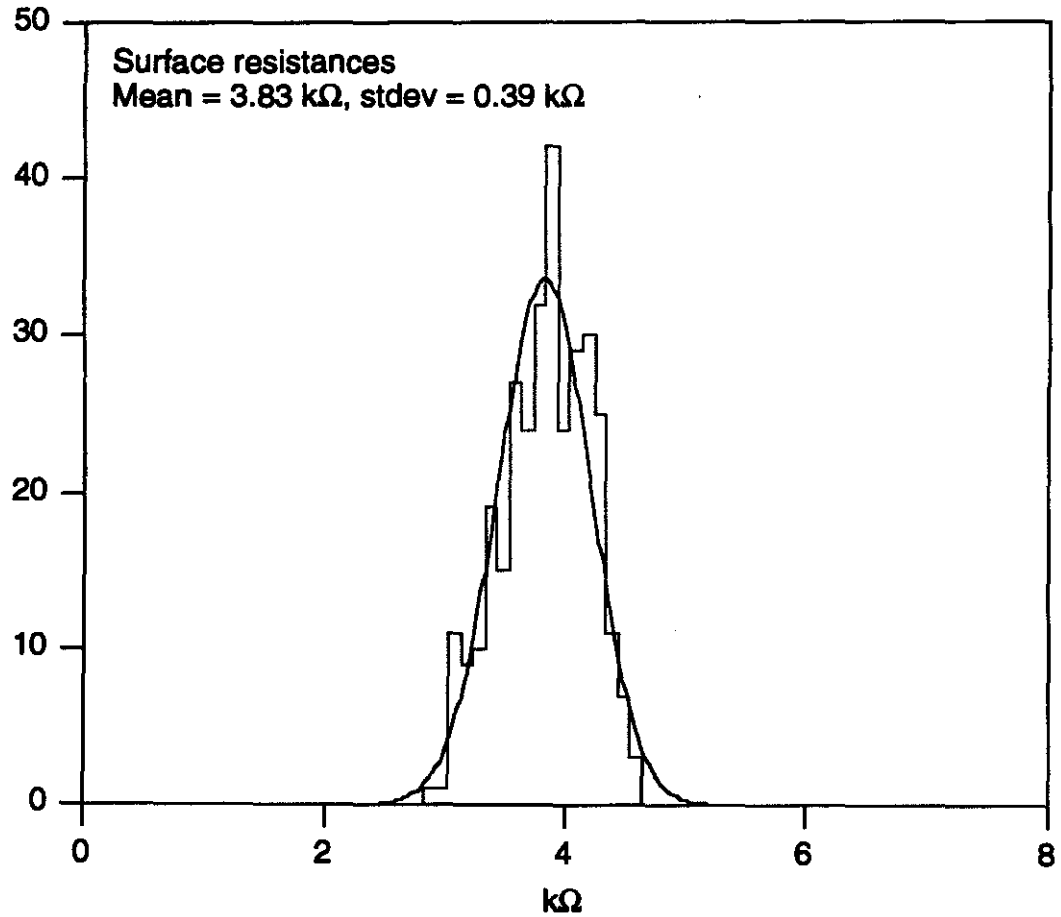

Figure 4. Resistance spectrum of graphite-coated profiles

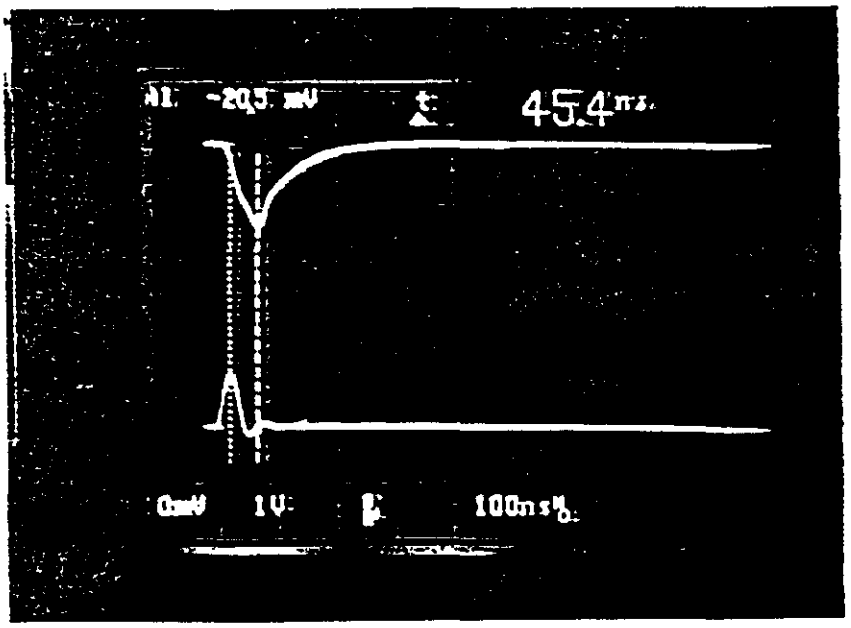

Figure 5. Typical output of the amplifier (upper trace). The input test pulse is shown in the lower trace.

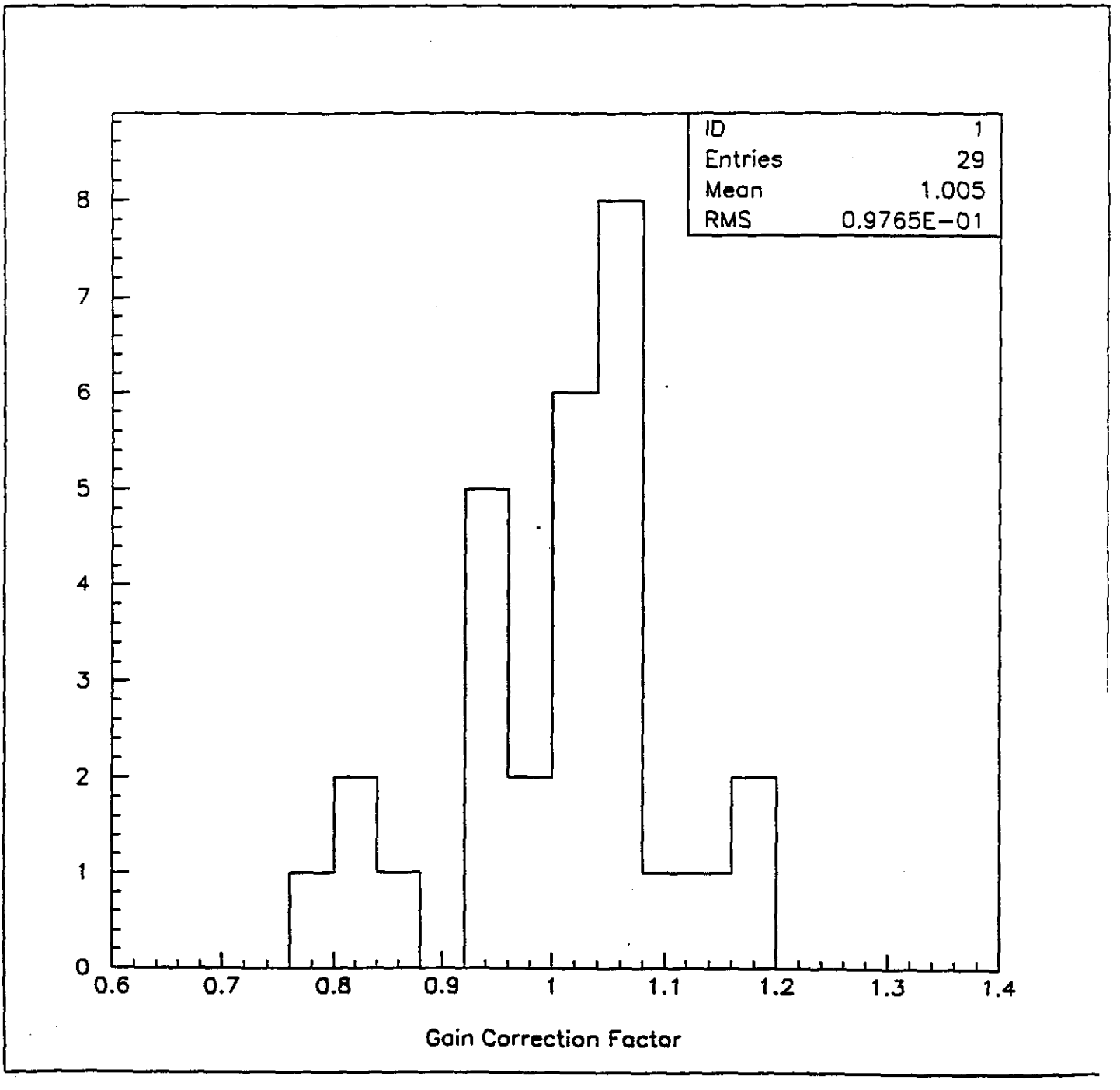

Figure 6. Relative gains of the preamplifiers.

Input file: runF0800 Events on File: 6932 groups on file: 4
Event#: 1795 Wed, Nov 25, 1992 5:33

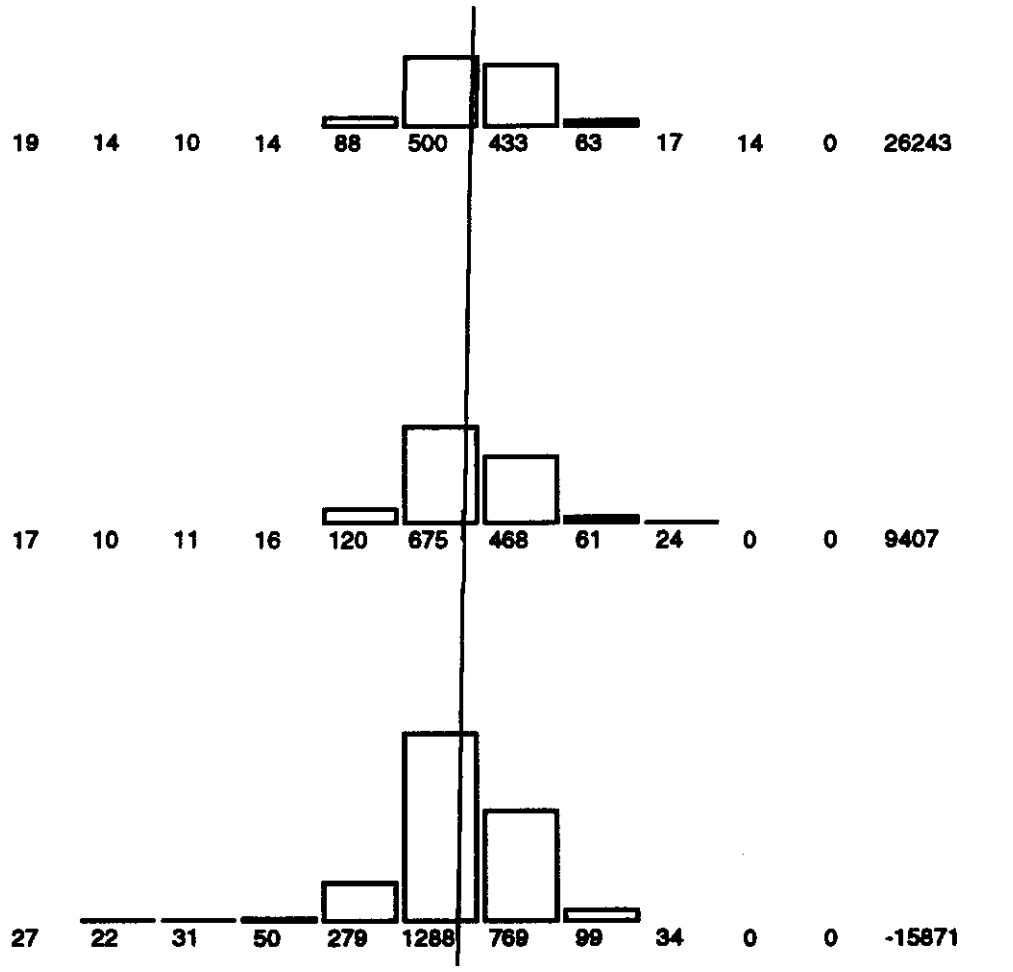

Residuals [μm]: 6.4 -12.9 6.4 Events/s: 75
Centroid [mm]: 29.142 28.747 28.315
Σ counts: 1084 1324 2435 Σ unused: 55 61 103 Angle: 0.9 °

Figure 7. Display of a typical cosmic muon event

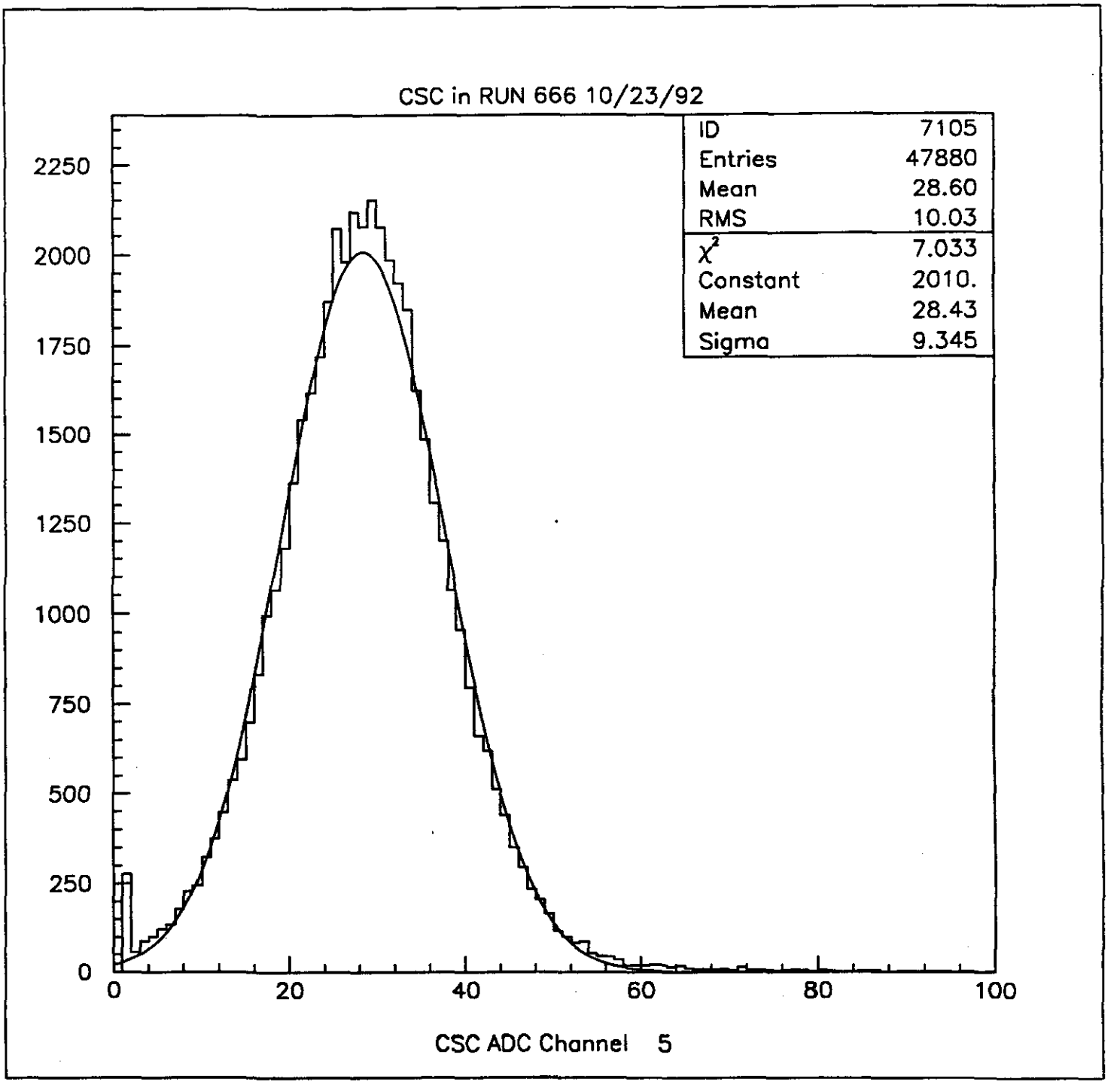

Figure 8. Pulse height spectrum for ADC channel #5 for all triggers.

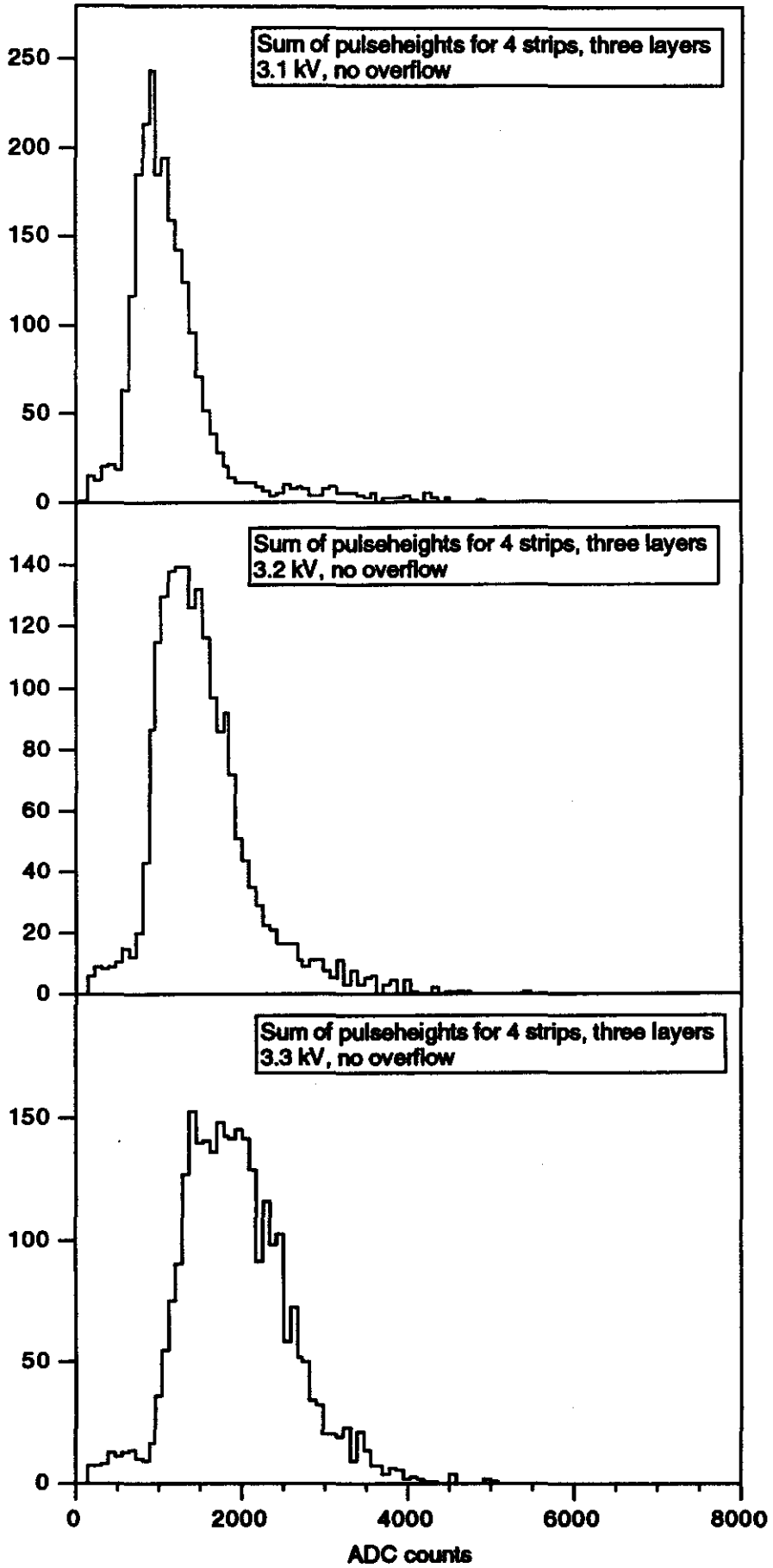

Figure 9. Pulse height spectra as a function of high voltage

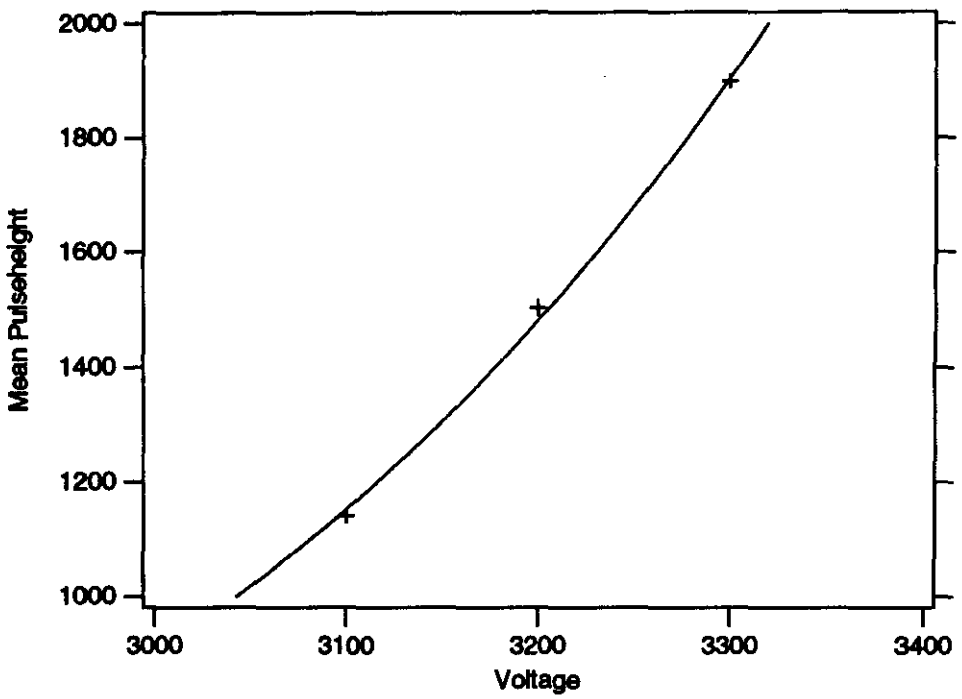

Figure 10. Mean pulse height as a function of high voltage

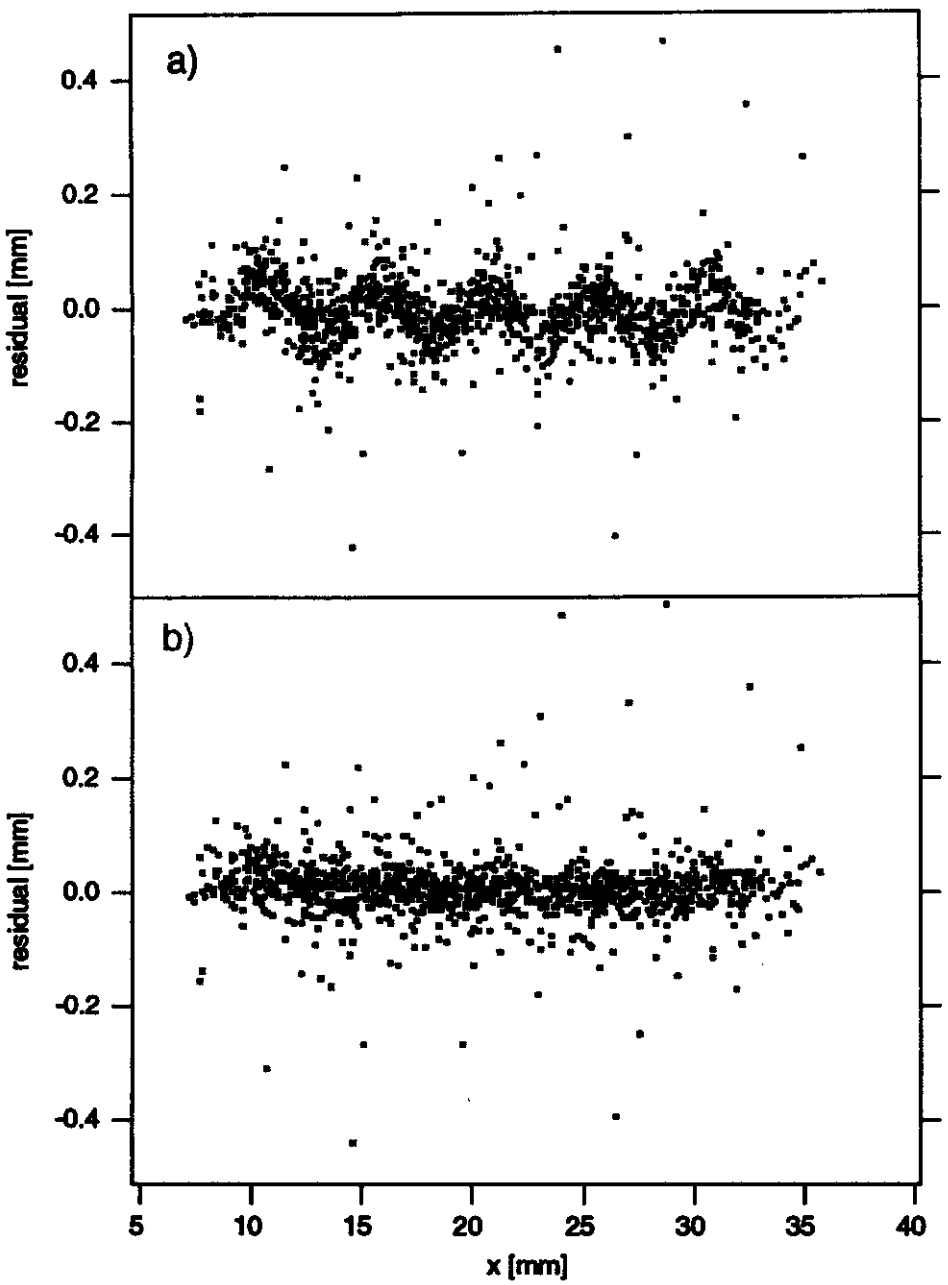

Figure 11. Residuals in the middle layer as a function of x before (a) and after (b) applying systematic corrections

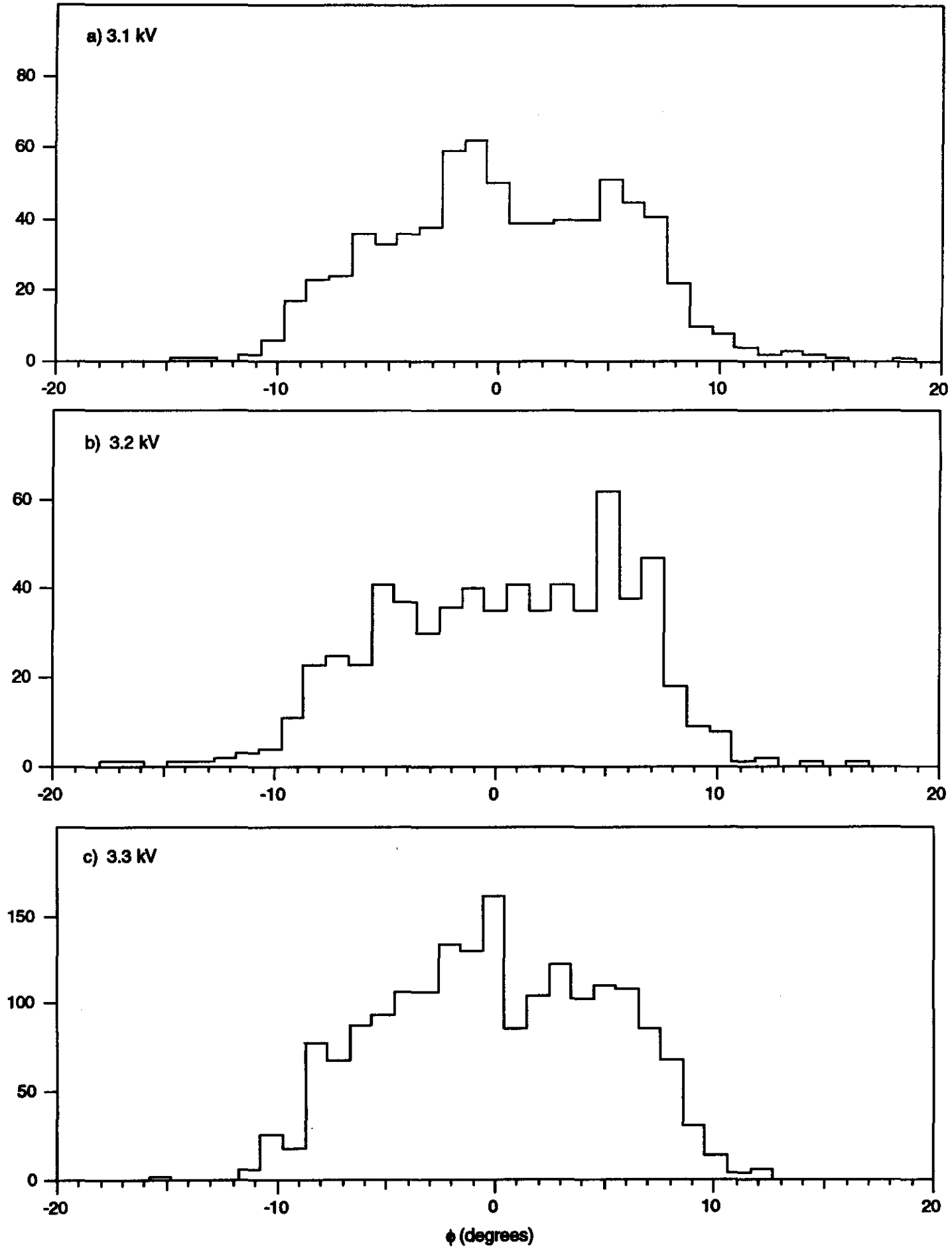

Figure 12. Angular distribution of reconstructed muon tracks for 3.1, 3.2, and 3.3 kV

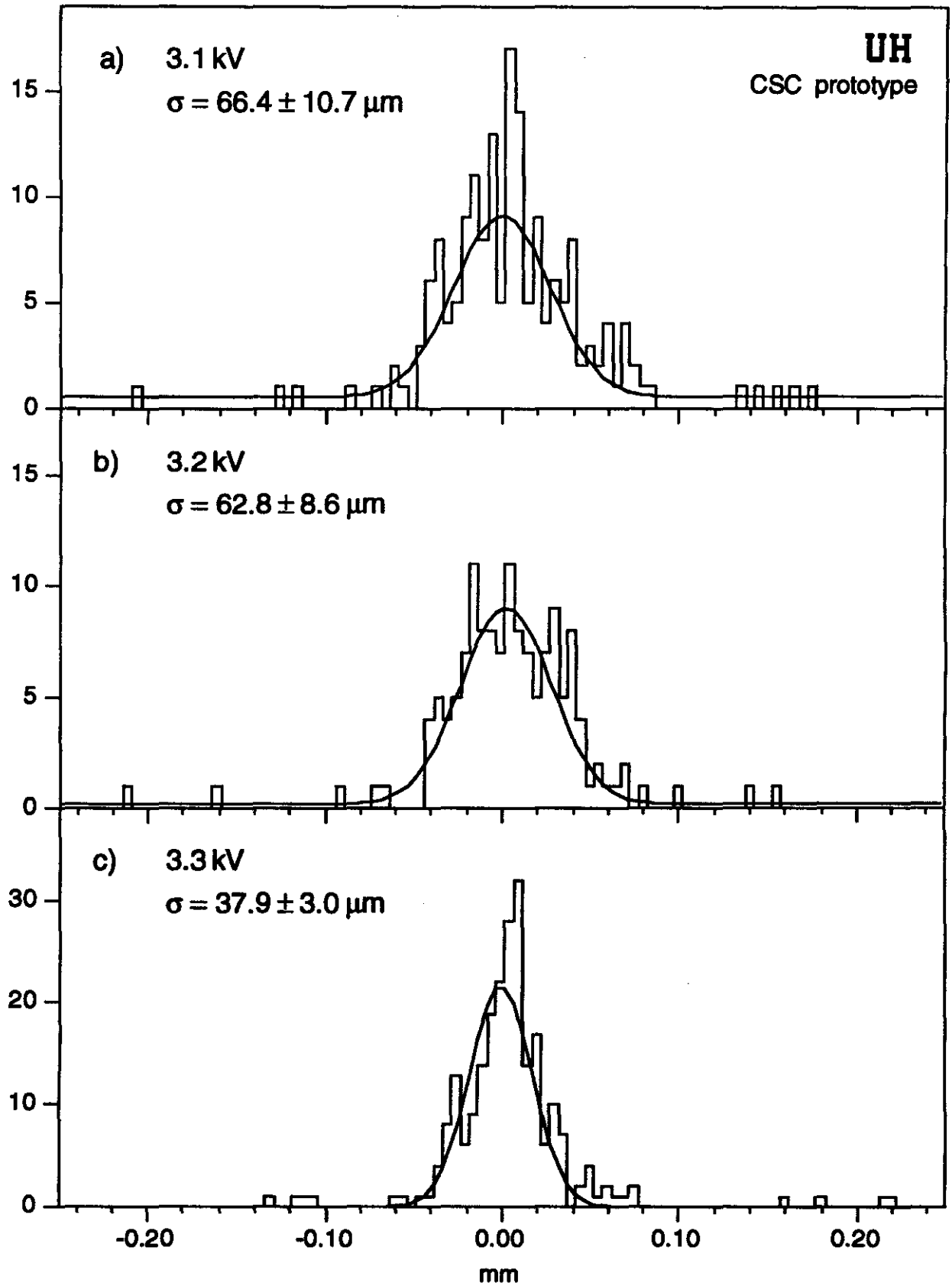

Figure 13. Single-layer spatial resolution for $|\phi| < 2°$ for 3.1, 3.2, and 3.3 kV

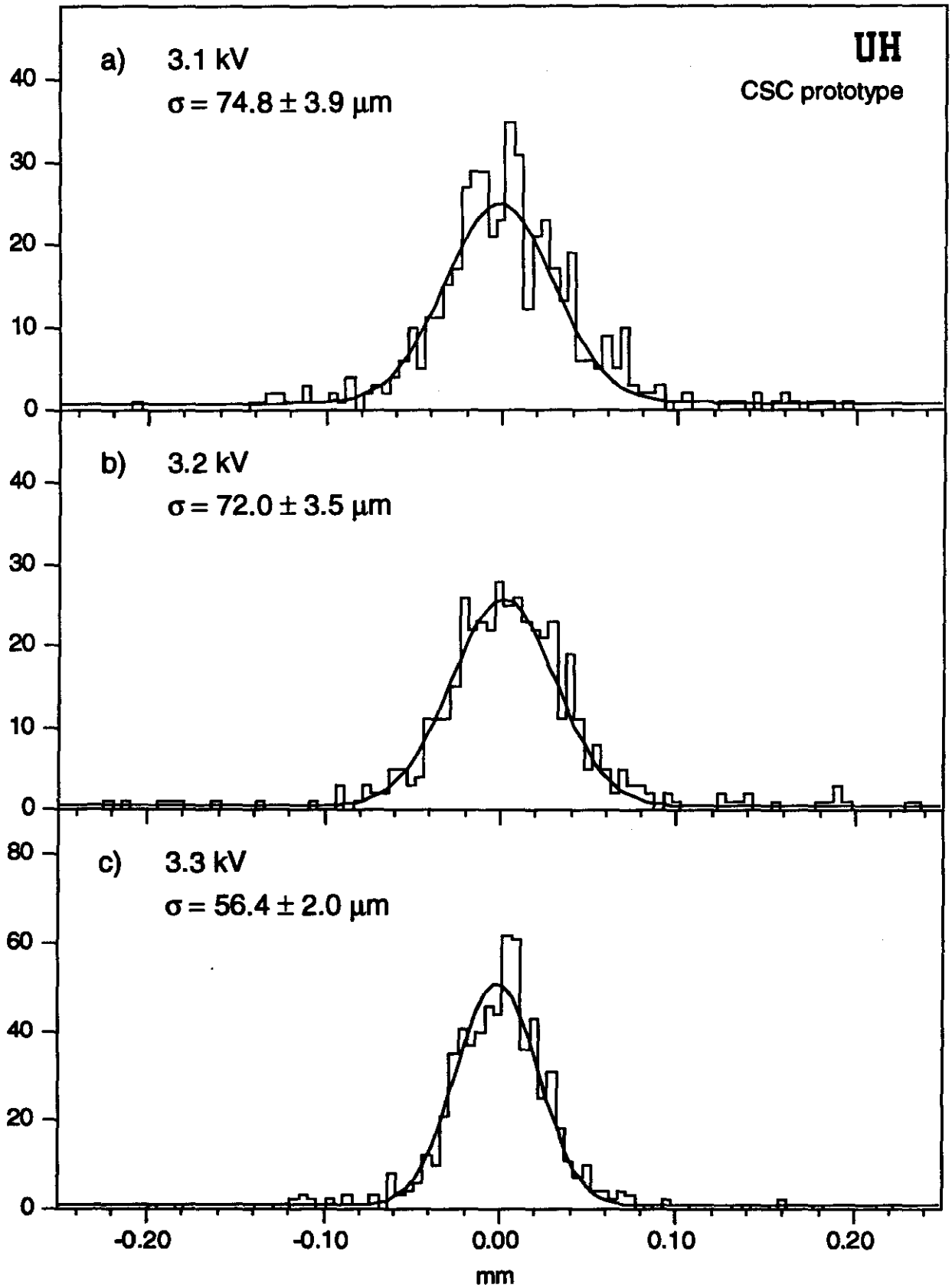

Figure 14. Single-layer spatial resolution for $|\phi| < 6°$ for 3.1, 3.2, and 3.3 kV